Thermophoresis of charged colloidal particles

Sébastien Fayolle, Thomas Bickel, and Alois Würger
CPMOH, Université Bordeaux 1 & CNRS, 351 cours de la Libération, 33405 Talence, France
(Received 28 November 2007; published 16 April 2008)

Thermally induced particle flow in a charged colloidal suspension is studied in a fluid-mechanical approach. The force density acting on the charged boundary layer is derived in detail. From Stokes' equation with no-slip boundary conditions at the particle surface, we obtain the particle drift velocity and the thermophoretic transport coefficients. The results are discussed in view of previous work and available experimental data.

DOI: 10.1103/PhysRevE.77.041404 PACS number(s): 82.70.−y, 66.10.C−

I. INTRODUCTION

A thermally driven flow, or Ludwig-Soret effect, is observed when applying a temperature gradient to gaseous or liquid phases [1–6]. The corresponding mass transport is relevant for natural and technological processes, such as the global circulation of sea water [7] and the phase behavior of eutectic systems at solidification [8]. In recent years, detailed experimental studies on macromolecular solutions and colloidal suspensions have revealed unambiguous and often surprising dependencies of the Soret effect on system parameters such as salinity, surface coating, solute concentration, and molecular weight [9–21]. Although the analogy to electrophoresis indicates the relevance of surface forces and suggests a hydrodynamic treatment [22,23], the physical mechanisms that drive thermophoresis in liquids are poorly understood and differ from those in gaseous phases [5,6].

Applying a generalized force such as an electric field or a thermal gradient to complex fluids results in a flow of heat, charge, particles. For sufficiently weak forces, such a nonequilibrium system is described in terms of linear force-current relations [1]. If the number density n and the temperature T are the relevant variables, the particle current in a dilute colloidal suspension reads

$$\mathbf{J} = -D\,\nabla n - nD_T\,\nabla T. \tag{1}$$

The first term on the right-hand side corresponds to Fick's law with the Einstein diffusion coefficient D, whereas the second one describes the thermally induced flow, with the thermal diffusion coefficient D_T. Equation (1) is completed by the expression for the heat current $\mathbf{J}_Q = -\kappa\nabla T - \kappa_n \nabla n$, with the thermal conductivity κ and the reduced Dufour coefficient κ_n; the cross-coefficients κ_n and D_T are related by the Onsager reciprocal rules [1]. The present work is concerned with the thermophoretic coefficient D_T of a charged colloidal suspension.

For a closed system the stationary state is characterized by $\mathbf{J}=0$; according to Eq. (1) a thermal gradient imposes an inhomogeneous density. Experimentally, D_T is determined by applying a temperature gradient to a uniform suspension ($\nabla n=0$) and by recording the initial current $\mathbf{J}=-nD_T\nabla T$, or by measuring the density modulation $\delta n=-n(D_T/D)\delta T$ induced by a temperature inhomogeneity δT in the steady state $\mathbf{J}=0$ [4]. The latter method gives the Soret coefficient $S_T = D_T/D$.

Equation (1) provides a macroscopic description for the particle current [1]. In order to obtain a relation between the kinetic coefficient D_T and the properties of solute and solvent, we split the particle current in two terms,

$$\mathbf{J} = n\mathbf{u} - \mu\,\nabla\,\Pi. \tag{2}$$

The first one accounts for the phoretic velocity $\mathbf{u}$ due to the interactions at the solute-solvent interface; this is a single-particle effect, i.e., it is independent of the density n and proportional to the thermal gradient,

$$\mathbf{u} = -C\,\nabla\,T. \tag{3}$$

The main purpose of this paper is to work out the proportionality factor C, similar to the coefficients obtained for an electric field or a chemical gradient [23]. The second term of $\mathbf{J}$ arises from the gradient of the osmotic pressure Π, with the mobility $\mu=1/(6\pi a\eta)$ depending on the solvent viscosity η and on the particle size a. The stationary state $\mathbf{J}=0$ provides the equilibrium condition where all forces acting on a given particle cancel. Inserting the single-particle velocity $\mathbf{u}=-C\nabla T$ and the osmotic pressure of a dilute suspension $\Pi=nk_BT$ in Eq. (2), and comparing this expression to Eq. (1), we find the Einstein relation $D=\mu k_BT$ and the thermodiffusion coefficient

$$D_T = \mu k_B + C. \tag{4}$$

For the Soret coefficient one has

$$S_T = \frac{1}{T}\left(1 + \frac{C}{\mu k_B}\right). \tag{5}$$

In the absence of particle-solvent interactions one has $C=0$ and $S_T=1/T$. This simply means that, at constant pressure, the stationary density is inversely proportional to the nonuniform temperature and that the particles accumulate in colder regions; this behavior is expected in the absence of solute-solvent interaction, where the suspended particles may be viewed as an ideal gas. Yet most colloidal suspensions show a considerably stronger, positive or negative, Soret effect, i.e., the interaction driven current $-nC\nabla T$ by far exceeds the ideal-gas term $-n\mu k_B\nabla T$ and may be directed toward colder or warmer regions. These deviations express the failure of the ideal-gas picture for the solute and emphasize the importance of particle-solvent interactions.

The properties of aqueous colloidal suspensions are largely dominated by charge effects. Besides the surface

charge density, the most important control parameters are the particle radius a and the Debye length λ. Recent measurements on suspensions of micelles and polystyrene nanoparticles [14,20,21,24,25] reported the laws $S_T \propto a\lambda^2$ or $\propto a^2\lambda$, depending on the experimental conditions and parameters. So far there is no generally accepted picture for the physical mechanisms at work; theoretical approaches based on either the free energy of the charged double layer or a hydrodynamic treatment give diverging results [20–22,26–31].

The present work deals with weakly charged particles, in the usual framework of driven transport in colloidal suspensions [23]. Section II gives a detailed derivation of the force density induced by the thermal gradient in the vicinity of a charged surface. In Sec. III we set up the hydrodynamic description and obtain the fluid and particle velocities; Sec. IV gives the thermodiffusion coefficient D_T. In Sec. V we compare our results with previous work and experimental data, and discuss the importance of the hydrodynamic boundary conditions.

II. THERMALLY INDUCED FORCE

The hydrodynamic treatment given in the following sections relies essentially on the force $\mathbf{f}dV$ exerted by the surface charge of the particle on a volume element dV of the surrounding fluid. The force density $\mathbf{f}$ is finite only within a boundary layer of thickness λ. Throughout this paper we suppose that λ is much smaller than the particle radius a,

$$\lambda \ll a. \tag{6}$$

Thus the hydrodynamic quanitites vary rapidly in the normal direction, and much more slowly along the interface. Here we evaluate the electric force density $\mathbf{f}$ that arises from a thermal gradient.

A. Electrostatics in the boundary layer

We consider a spherical particle of charge Q and radius a. It is convienent to define the charge density $\sigma = Q/(4\pi a^2)$. The surface charge modifies the properties of the fluid in the boundary layer in several respects. First, it results in an electric field $\mathbf{E} = -\boldsymbol{\nabla}\psi$; the resulting stress is accounted for in terms of the Maxwell tensor

$$\mathcal{T}_{ij} = \varepsilon\left(E_i E_j - \frac{1}{2}E^2\delta_{ij}\right).$$

Second, the electrostatic potential ψ is screened through the accumulation of mobile counterions in the electrolyte. In mean-field approximation, the excess densities of (monovalent) positive and negative ions are given by

$$n_\pm = n_0(e^{\mp e\psi/k_BT} - 1),$$

where n_0 is the salinity. As a result the fluid in the boundary layer carries a charge density

$$\rho = e(n_+ - n_-)$$

and an excess density of mobile ions

$$n = n_+ + n_-.$$

Accordingly, the force $\mathbf{f}(\mathbf{r})dV$ acting on a volume element dV of the fluid comprises two terms,

$$\mathbf{f} = \boldsymbol{\nabla}\cdot\mathcal{T} - \boldsymbol{\nabla}(nk_BT), \tag{7}$$

where the divergence of the Maxwell tensor $\boldsymbol{\nabla}\cdot\mathcal{T}$ arises from the electric field, and the entropic force $-\boldsymbol{\nabla}(nk_BT)$ from the nonuniform osmotic pressure. The former term may be rewritten by using the definition of the displacement vector $\mathbf{D} = \varepsilon\mathbf{E}$, its relation to the charge density $\rho = \boldsymbol{\nabla}\cdot\mathbf{D}$, and the fact that the curl of the electric field $\mathbf{E} = -\boldsymbol{\nabla}\psi$ vanishes, $\boldsymbol{\nabla}\times\mathbf{E} = 0$. Thus one finds the well-known force density acting on a charged dielectric body [32,33],

$$\boldsymbol{\nabla}\cdot\mathcal{T} = \rho\mathbf{E} - \frac{1}{2}E^2\,\boldsymbol{\nabla}\,\varepsilon, \tag{8}$$

where $\rho\mathbf{E}$ describes the action of the electric field, and the remainder accounts for the dielectrophoretic force due to the spatial variation of the permittivity [32]. The additional contribution to Eq. (7) arises from the osmotic pressure of the mobile ions, i.e., from the fact that a charged fluid is a conductor.

B. Debye-Hückel approximation

The present work is restricted to the case of weak surface charges, where the potential energy of a mobile ion is smaller than the thermal energy,

$$e\psi \ll k_BT. \tag{9}$$

Moreover, Eq. (6) implies that the Debye screening length

$$\lambda = \sqrt{\frac{\varepsilon k_BT}{2n_0e^2}}$$

is much smaller than the particle size.

Under the assumption (9) the ion densities $n_\pm$ may be expanded to quadratic order in the small parameter $e\psi/k_BT$. Then the charge density is linear in the potential, $\rho = -\varepsilon\psi/\lambda^2$, and the electric force in Eq. (7) becomes

$$\rho\mathbf{E} = \frac{\varepsilon\psi}{\lambda^2}\,\boldsymbol{\nabla}\,\psi = \frac{\varepsilon}{2\lambda^2}\,\boldsymbol{\nabla}\,\psi^2.$$

With the definition of the Debye length, the leading term of the excess pressure reads as $nk_BT = (\varepsilon\psi^2/2\lambda^2)$, and its gradient may be rewritten as

$$\boldsymbol{\nabla}(nk_BT) = \frac{\varepsilon}{2\lambda^2}\,\boldsymbol{\nabla}\,\psi^2 - \frac{\varepsilon\psi^2}{2\lambda^2}\frac{\boldsymbol{\nabla}T}{T}.$$

Inserting these terms in Eq. (7) we get

$$\mathbf{f} = -\frac{1}{2}E^2\,\boldsymbol{\nabla}\,\varepsilon + \frac{\varepsilon\psi^2}{2\lambda^2}\frac{\boldsymbol{\nabla}T}{T}. \tag{10}$$

So far we have not used the precise form of the electrostatic potential. The force $\mathbf{f}$ solely depends on the gradients of the permittivity ε and the nonuniform temperature $T(\mathbf{r})$.

Since this work is confined to the case of a thin boundary layer, $\lambda \ll a$, we use the screened electrostatic potential of a flat surface

$$\psi = \psi_0 e^{-z/\lambda}, \quad \psi_0 = \frac{\lambda \sigma}{\varepsilon}. \tag{11}$$

Taking the derivative with respect to the normal coordinate gives the electric field $E=\psi/\lambda$. The charge density of the fluid reads $\rho=-(\sigma/\lambda)e^{-z/\lambda}$; one readily verifies $\int dz\rho=-\sigma$, i.e., the overall charge of the double layer is zero.

Comparison with the surface potential of a spherical particle $Q/[4\pi\varepsilon(1+a/\lambda)a]=\psi_0/(1+\lambda/a)$ reveals that the finite curvature would result in corrections of the order λ/a. Since we rely on Eq. (6) throughout this paper, these corrections are of no significance.

C. Uniform temperature

We briefly address the force balance in a uniform system where the permittivity and the temperature are constants $\nabla T=0$. Clearly, Eq. (10) states that the total force vanishes, $\mathbf{f}=0$; yet each of the terms in Eq. (7) contains a finite contribution that is independent of ∇T. From the potential (11) one finds the force on the charged fluid,

$$\rho E_z = -\rho \partial_z \psi,$$

and the gradient of the entropic pressure,

$$k_B T \partial_z n = (\varepsilon/\lambda^2)\psi \partial_z \psi.$$

With the above expression for the charge density these terms cancel each other. This just means that for $\nabla T=0$ there is no net force and that the fluid is immobile.

D. Thermal force

Now we consider the effect of a small but finite temperature gradient. Since the permittivity gradient in Eq. (10) arises from the nonuniform temperature, $\nabla\varepsilon=(d\varepsilon/dT)\nabla T$, both contributions to the thermal force are already proportional to ∇T. In view of the linear current-force relation (1), terms of higher order in ∇T are irrelevant. Thus we calculate the coefficients in Eq. (10) from the unperturbed potential (11). In particular, this leads to the electric field $E=\psi/\lambda$; with the logarithmic derivative of the permittivity

$$\tau = -\frac{d \ln \varepsilon}{d \ln T}$$

we obtain the final form for the force field,

$$\mathbf{f} = \frac{\varepsilon \psi^2}{2\lambda^2}(1+\tau)\frac{\nabla T}{T}. \tag{12}$$

E. Temperature gradient

Due to the different heat conductivities of particle and solvent, the temperature field close to the particle surface differs from the externally applied uniform modulation [34]. In the Introduction, e.g., in Eq. (3), ∇T refers to the externally applied thermal gradient, i.e., to its value far from the particle, which we denote

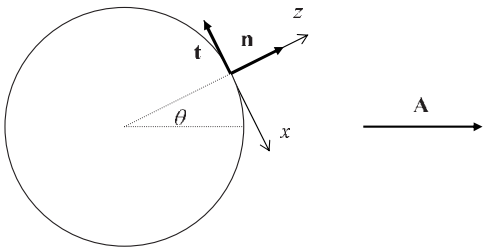

FIG. 1. Schematic view of a spherical particle of radius a in a temperature gradient $\mathbf{A}=\nabla T$. The surface charge density σ is screened by a diffuse layer of thickness $\lambda \ll a$. At the surface the local coordinates x,z and the normal and tangent vectors $\mathbf{n},\mathbf{t}$ are indicated.

$$\mathbf{A} = \nabla T|_\infty$$

in the remainder of this paper. On the other hand, Eq. (12) involves the gradient close to the particle surface. Since heat propagation is much faster than particle migration, the temperature field may be taken as stationary. The heat conduction equation for a spherical particle is readily solved, and the tangential component of the thermal gradient at the particle surface reads [35]

$$\partial_x T = -\xi(\mathbf{t}\cdot\mathbf{A}) = \xi A \sin\theta. \tag{13}$$

As shown in Fig. 1, θ denotes the angle between the surface normal $\mathbf{n}$ and the applied gradient $\mathbf{A}$. According to the usual definition of polar coordinates, the tangent vector $\mathbf{t}$ coincides with the negative x axis. The parameter $\xi=3\kappa_S/(2\kappa_S+\kappa_P)$ is determined by the ratio of the heat conductivities of solvent and particle. As to the normal component, one finds

$$\partial_z T = \xi_n(\mathbf{n}\cdot\mathbf{A}) = \xi_n A \cos\theta$$

with a modified prefactor $\xi_n=3\kappa_P/(2\kappa_S+\kappa_P)$.

The unperturbed temperature gradient reads in local coordinates $A_x=A\sin\theta$ and $A_z=A\cos\theta$. Thus the changes at the surface of a colloidal particle are expressed by the factors ξ and ξ_n. For the case where the heat conductivities of solute and solvent are identical, $\kappa_S=\kappa_P$, we have $\xi=1=\xi_n$, i.e., the thermal gradient is constant everywhere, $\nabla T=\mathbf{A}$.

III. HYDRODYNAMICS

The particle velocity $\mathbf{u}$ has to be derived from a fluid-mechanical treatment [23]. The thermally driven motion of micron or nanometer sized particles in a viscous liquid involves small Reynolds numbers, i.e., inertia effects are negligible. Then the stationary velocity is given by Stokes' equation [35],

$$\eta\nabla^2\mathbf{v} = \nabla P - \mathbf{f}, \tag{14}$$

where η is the solvent viscosity, P is the hydrostatic pressure, and $\mathbf{f}$ is the force density exerted by the particle on the fluid. An incompressible fluid satisfies $\nabla\cdot\mathbf{v}=0$, and in gen-

eral stick boundary conditions are supposed to apply at the particle surface,

$$\mathbf{v}|_{r=a} = \mathbf{u}. \tag{15}$$

The characteristic length scales of the normal and parallel derivatives in Eq. (14) are given by λ and a. The condition of a thin boundary layer, as expressed in Eq. (6), thus implies that the forces vary rapidly in the normal direction, and much more slowly along the interface. The resulting separation of length scales permits us to calculate the particle velocity in two steps. First, resorting to a one-dimensional (1D) approximation that is valid at distances much shorter than the particle size, we derive the boundary velocity induced by the thermal force. In a second step we match this solution with that of the force-free Stokes equation at distances well beyond λ, and thus obtain the fluid velocity field.

In the laboratory frame the particle moves at speed $\mathbf{u}$ and the fluid velocity vanishes at infinity. For the sake of computational simplicity, we transform to the reference frame in which the particle is at rest. Indicating the corresponding velocities by a hat, we have $\hat{\mathbf{u}}=0$ and

$$\hat{\mathbf{v}}(\mathbf{r}) = \mathbf{v}(\mathbf{r}) - \mathbf{u}.$$

For the fluid motion in the boundary layer, local coordinates x and z turn out to be most convenient, whereas the velocity field at larger distances is best described in terms of polar coordinates r and θ with the origin at the particle center; see Fig. 1.

A. Boundary layer

We rewrite Eq. (14) in terms of the normal and parallel coordinates z and x,

$$\eta \boldsymbol{\nabla}^2 \hat{v}_i = \partial_i P - f_i,$$

with $\partial_x = \partial/\partial x$, etc., and where $\hat{\mathbf{v}}$ is the relative fluid velocity with respect to the particle surface. The normal component vanishes close to the interface, $\hat{v}_z=0$, which implies $\partial_z P - f_z = 0$ [23]. Since the force $\mathbf{f}$ is finite within the boundary layer only, the hydrostatic pressure is constant at larger distances. Integrating $\partial_z P = f_z$ we have

$$P = P_0 - \int_z^\Lambda dz' f_z(z'), \tag{16}$$

where P_0 is a constant. The upper bound of the integral is much larger than the thickness of the boundary layer but much smaller than the particle size, and thus satisfies

$$\lambda \ll \Lambda \ll a.$$

Regarding the tangential velocity $\hat{v}_x$, its derivative along the surface is much smaller than the normal component, resulting in the inequality $\partial_x^2 \hat{v}_x \ll \partial_z^2 \hat{v}_x$. Discarding $\partial_x^2 \hat{v}_x$ accordingly, the equation for the tangential velocity component becomes

$$\eta \partial_z^2 \hat{v}_x = \partial_x P - f_x. \tag{17}$$

The derivative on the right-hand side gives the lateral force per unit volume exerted on the fluid. Integrating this relation once gives the shear stress $\sigma_{xz} = \eta \partial_z \hat{v}_x$. This quantity does not have a rigorous reference value, i.e., it takes finite values both at the particle surface and beyond the boundary layer. Yet in the boundary layer approximation, i.e., by assuming an infinite flat surface, σ_{xz} is zero well beyond the boundary layer. Taking $\sigma_{xz}(\Lambda)=0$ as reference value, the shear stress is given by its variation from Λ to a distance z from the surface,

$$\sigma_{xz}(z) = \int_z^\Lambda dz' (f_x - \partial_x P). \tag{18}$$

Integrating once more gives the velocity of the fluid with respect to the particle,

$$\hat{v}_x(z) = \frac{1}{\eta} \int_0^z dz' \sigma_{xz}(z'). \tag{19}$$

Here we have used stick boundary conditions, i.e., $\hat{v}_x(z)$ is zero at $z=0$.

B. Boundary velocity

Replacing the upper bound of the integral with $z \to \Lambda$, the quantity $v_x(\Lambda)$ gives the relative velocity of the fluid beyond the boundary layer with respect to the particle surface. Inserting the nonuniform pressure P one finds

$$v_B = \frac{1}{\eta} \int_0^\Lambda dz \int_z^\Lambda dz' \left(f_x + \frac{\partial}{\partial x} \int_{z'}^\Lambda dz'' f_z(z'') \right). \tag{20}$$

On a mesoscopic level the relevant length scale is given by the particle size a; because of $\Lambda \ll a$, one may consider the limit $\Lambda/a \to 0$ and take v_B as the fluid velocity at the interface.

This velocity depends on both components of the force density f_x and f_z. We show that for the electric force studied here, the latter contribution is negligible, i.e., the tangential derivative $\partial_x P$ of the pressure is small as compared to f_x. Indeed, if the thermal conductivities of solvent and particle are not very different, the normal and parallel temperature gradients $\partial_x T$ and $\partial_z T$ components are of the same order of magnitude, and so are the force components f_x and f_z. Since the force is finite within the boundary layer only, the second term in parentheses in Eq. (20) is approximately $\partial_x(\lambda f_z)$; this has to be compared with f_x. From Eq. (12) it is clear that $\partial_x(\lambda f_z)$ comprises terms proportional either to the square of the thermal gradient $\propto (\partial_x T)(\partial_z T)$ or to the second derivative $\propto \partial_x \partial_z T$. (The curvature of the temperature field vanishes in the bulk fluid, but is finite in the boundary layer.) The quadratic terms arise from the factors $\lambda, \varepsilon, \psi, T$ present in λf_z; they are not significant in view of the linear current-force relation (1). As to the second derivative, the above discussion of the thermal gradient implies that $\partial_x \partial_z T$ varies on the scale of the particle size, $\partial_x \partial_z T \sim (1/a) \partial_z T$. Thus we find that the second term in parentheses in Eq. (20) is at most of the order

$$\partial_x(\lambda f_z) \sim (\lambda/a) f_z \ll f_x.$$

As a consequence of this "boundary layer approximation" [23], we discard the integral term and we have

$$v_B = \frac{1}{\eta}\int_0^\Lambda dz \int_z^\Lambda dz' f_x.$$

Inserting the tangential component f_x in Eq. (20) and noting that only the electrostatic potential ψ depends on the integration variable, we obtain a double integral of ψ^2. With the above expression for ψ this integral is readily performed; putting $e^{-\Lambda/\lambda} \to 0$ one finds

$$\int_0^\Lambda dz \int_z^\Lambda dz' \psi^2 = \frac{\lambda^2 \psi_0^2}{4},$$

and thus the boundary velocity

$$v_B = \frac{\varepsilon \psi_0^2}{8\eta T}(1+\tau)\partial_x T.$$

The parallel component of the temperature gradient depends on the orientation of the surface with respect to **A**. Separating the resulting sine function, we have

$$v_B = v_0 \sin\theta,$$

with the constant

$$v_0 = \frac{\varepsilon \psi_0^2}{8\eta}(1+\tau)\frac{\xi A}{T}. \tag{21}$$

For later use we give the vector quantity in the basis related to polar coordinates,

$$\mathbf{v}_B = -v_0 \sin\theta \mathbf{t}, \tag{22}$$

where the minus arises since the tangent vector **t** points along the negative x axis.

C. Three-dimensional flow

The electric force and the boundary velocity have been evaluated in terms of a one-dimensional approximation to Stokes' equation that ceases at distances beyond Λ. In this range one has to deal with the 3D Stokes equation, albeit with modified boundary conditions. In a mesoscopic description, we may put $\Lambda/a \to 0$ and consider v_B as the fluid velocity at the interface. Thus Eq. (14) reduces to the force-free Stokes equation

$$\eta \nabla^2 \mathbf{v} = \nabla P. \tag{23}$$

Treating the fluid as incompressible imposes continuity of the normal component of the velocity,

$$\mathbf{n}\cdot(\mathbf{v}-\mathbf{u})|_{a+\Lambda} = 0. \tag{24}$$

A second condition is obtained by noting that there is no net external force acting on the system consisting of the particle and the charged fluid. Thus the integrated normal force outside the boundary layer vanishes [23],

$$\oint_{a+\Lambda} dS \boldsymbol{\sigma}\cdot\mathbf{n} = 0, \tag{25}$$

where the stress tensor

$$\boldsymbol{\sigma} = \boldsymbol{\sigma}' - P$$

comprises the dissipative term or viscous force density $\sigma'_{ij} = \eta(\partial_i v_j + \partial_j v_i)$, and the hydrostatic pressure P [35]. The third condition involves the velocity (22), which accounts for the force acting on the double layer,

$$\mathbf{t}\cdot(\mathbf{v}-\mathbf{u})|_{a+\Lambda} = \mathbf{t}\cdot\mathbf{v}_B. \tag{26}$$

We transform to the reference frame in which the particle is at rest, with $\hat{\mathbf{u}}=0$ and $\hat{\mathbf{v}}(\mathbf{r})=\mathbf{v}(\mathbf{r})-\mathbf{u}$. The solution of Stokes' equation at small Reynolds numbers in spherical coordinates $\hat{\mathbf{v}}=\hat{v}_r\mathbf{n}+\hat{v}_\theta\mathbf{t}$ reads [35]

$$\hat{v}_r = -u\cos\theta\left(1 - 2\alpha\frac{a}{r} + 2\beta\frac{a^3}{r^3}\right), \tag{27a}$$

$$\hat{v}_\theta = u\sin\theta\left(1 - \alpha\frac{a}{r} - \beta\frac{a^3}{r^3}\right), \tag{27b}$$

where θ is the polar angle with respect to the x axis and the radial and tangential unit vectors $\mathbf{n}=\mathbf{r}/r$ and $\mathbf{t}=\partial\mathbf{n}/\partial\theta$. This flow field is related to a nonuniform hydrostatic pressure

$$P(\mathbf{r}) = P_0 + \alpha\frac{2\eta u a}{r^2}\cos\theta\,.$$

The parameters u, α, β are determined from the solution of Stokes with the boundary conditions (24)–(26).

The first two of these conditions involve the fluid velocity and stress only. In the particle-fixed frame the normal velocity vanishes, $\hat{v}_r|_{r=a}=0$, resulting in $1-2\alpha+2\beta=0$. The total stress at the interface can be written as $\boldsymbol{\sigma}\cdot\mathbf{n}=\mathbf{n}\sigma_{rr}+\mathbf{t}\sigma_{r\theta}$, with the entries of the dissipative part in spherical coordinates [35]

$$\sigma'_{rr} = 2\eta\frac{\partial\hat{v}_r}{\partial r}, \quad \sigma'_{r\theta} = \eta\left(\frac{\partial\hat{v}_\theta}{\partial r} - \frac{\hat{v}_\theta}{r}\right). \tag{28}$$

Integrating Eq. (25) over a sphere just outside the boundary layer gives the relation $1-5\alpha+2\beta=0$. One readily obtains the amplitudes of the velocity field varying with distance as $1/r$ and $1/r^3$, respectively,

$$\alpha = 0, \quad \beta = -\frac{1}{2}. \tag{29}$$

Taking the back transformation $\mathbf{v}(\mathbf{r})=\hat{\mathbf{v}}(\mathbf{r})+\mathbf{u}$ yields the fluid velocity in the laboratory frame,

$$\mathbf{v}(\mathbf{r}) = u\frac{a^3}{r^3}\left(\frac{1}{2}\sin\theta\mathbf{t} + \cos\theta\mathbf{n}\right). \tag{30}$$

Finally we determine the particle velocity u. With Eq. (22) and $\Lambda \to 0$, the remaining condition (26) reads

$$-v_0\sin\theta = \hat{v}_\theta|_{a+\Lambda}.$$

Inserting $\hat{v}_\theta$ we have $u=-\frac{2}{3}v_0$ and, with the expression for v_0,

$$u = -\xi\frac{\varepsilon\psi_0^2}{12\eta T}(1+\tau)A. \tag{31}$$

The maximum value of the boundary velocity v_B occurs at $\theta=\frac{\pi}{2}$ and exceeds the particle velocity, i.e., the particle and

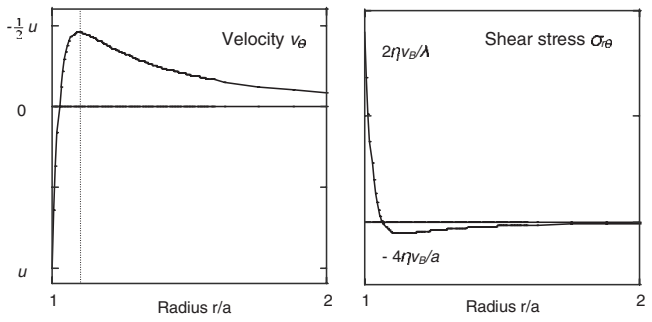

FIG. 2. Schematic plot of the tangential velocity v_θ and the shear stress $\sigma_{r\theta}$ for $\theta=\frac{\pi}{2}$ and $a\leq r\leq 2a$. The vertical dashed line indicates the thickness of the boundary layer, i.e., the Debye length λ. The minimum and maximum values of v_θ and $\sigma_{r\theta}$ are indicated.

the fluid beyond the boundary layer move in opposite directions.

D. Boundary layer approximation

The expression (20) relies on two assumptions: slow variation of the tangential velocity in the boundary layer, $\partial_x^2\hat{v}_x \ll \partial_z^2\hat{v}_x$, and a small shear stress beyond a distance Λ. Here we justify these assumptions by evaluating the quantities from the 3D solution, and we summarize the variation of the velocity field and the shear stress from the particle surface to distances well beyond the boundary layer.

The parallel derivative of the velocity in the boundary layer $\partial_x\hat{v}_x$ matches $(1/a)\partial_\theta\hat{v}_\theta$; according to Eq. (30) it is of the order v_θ/a. Comparing to the normal derivative in the boundary layer $\partial_z\hat{v}_x\sim\hat{v}_x/\lambda$, one readily verifies $\partial_x\hat{v}_x \ll \partial_z\hat{v}_x$, i.e., that the latter provides the dominant contribution in terms of the small parameter λ/a; the same argument applies to the second derivative.

In Eq. (18) we have used that for a flat surface, the shear stress vanishes beyond the boundary layer. From Eqs. (27) and (28) one obtains

$$\sigma_{r\theta}|_{a+\Lambda} = -\frac{2}{a}\eta v_B,$$

the shear stress is proportional to the inverse curvature radius of the particle. The variation of the shear stress through the boundary layer is given by putting $z=0$ in Eq. (18),

$$\sigma_{xz}(0) = \frac{2}{\lambda}\eta v_B.$$

One readily finds that $\sigma_{r\theta}|_{a+\Lambda}$ is by a factor λ/a smaller than the term retained in Eq. (18). These relations confirm the validity of the boundary layer approximation in the case $\lambda \ll a$.

In Fig. 2 we plot schematically the variation of both the velocity field and the shear stress. In view of Eq. (31) we put $u<0$, i.e., the particle moves in the direction opposite to the thermal gradient. The left panel shows the function $v_\theta(r)$ at $\theta=\frac{\pi}{2}$, i.e., in the plane normal to the applied thermal gradient where the radial component is zero and where the relative velocity reads $v_B=-\frac{3}{2}u$. At the particle surface the fluid velocity takes the value $v_\theta|_a=u$, increases through the boundary layer, and attains $v_\theta|_{a+\Lambda}=-\frac{1}{2}u$. At larger distances, the velocity vanishes with the characteristic power law $v_\theta=-\frac{1}{2}u(a/r)^3$. The shear stress is shown in the right panel. Its maximum and minimum values occur at the particle surface and beyond the boundary layer, respectively, and they differ by a factor λ/a. At larger distances the shear stress vanishes as $\sigma'_{r\theta}\sim 1/r^4$.

IV. PHORETIC COEFFICIENTS

Equation (31) gives the phoretic velocity of the suspended particle in terms of the applied thermal gradient and thus defines the proportionality factor in Eq. (3)

$$C = \xi(1+\tau)\frac{\varepsilon\psi_0^2}{12\eta T}. \tag{32}$$

The transport coefficient D_T is obtained from Eq. (4), with the mobility $\mu=1/(6\pi\eta a)$ and the ratio of heat capacities $\xi=3\kappa_S/(2\kappa_S+\kappa_P)$,

$$D_T = \frac{k_B}{6\pi\eta a} + \frac{\kappa_S}{2\kappa_S+\kappa_P}(1+\tau)\frac{\varepsilon\psi_0^2}{4\eta T}. \tag{33}$$

The first term depends on the particle size a; for sufficiently large solutes it is negligible, and D_T is independent of the particle size. For a polymer coil, a has to be replaced by the gyration radius R.

Most experiments study the stationary density modulation $\delta n/n=-(D_T/D)\delta T$ induced by the temperature inhomogeneity δT, and thus measure the Soret coefficient $S_T=D_T/D$ rather than the transport coefficient D_T. With $D=k_BT/(6\pi\eta a)$ one has

$$S_T = \frac{1}{T}\left(1+\xi(1+\tau)\frac{\pi a\varepsilon\psi_0^2}{2k_BT}\right). \tag{34}$$

The first term in brackets gives the ideal-gas expression $S_T=1/T$; the remaining one is proportional to the particle size a. For solutes larger than a few nanometers, phoretic motion due to surface forces in general exceeds the diffusive term, i.e., the coefficient C is larger than μk_B. In this limit the above quantities vary with the square of the Debye length. The Soret coefficient reads

$$S_T \propto \lambda^2 a, \tag{35}$$

whereas $D_T\propto\lambda^2$ and $u\propto\lambda^2$ are independent of the particle size.

V. DISCUSSION

A. Approximations

Our results follow from a hydrodynamic treatment of the fluid surrounding a charged particle. In view of the discrepancies with recent work discussed below, it seems worthwhile to review the underlying assumptions.

(i) The surface charge density σ is supposed to be constant, resulting in a surface potential ψ_0 that depends only weakly on temperature through the permittivity and the

screening length. For most experimental systems, the charge σ arises from ionic surfactants grafted on a particle or trapped at a liquid interface. If the degree of dissociation of this surfactant varied with T, the value of the surface charge σ and thus the potential ψ_0 would show an additional temperature dependence.

(ii) The present work relies on the validity of the Debye-Hückel approximation, i.e., on sufficiently small surface charges. Yet for several systems the measured values of S_T indicate effective valencies Z close to the value $Z^* = (4a^2/\ell_B)(1+\lambda/a)$ where the weak-coupling assumption ceases to be valid [36].

(iii) Both the hydrodynamic treatment and the electrostatics are restricted to the leading order in powers of the parameter λ/a. For micron-size particles this ratio is of the order of a few percent [20,21] yet approaches unity for micelles and water-in-oil droplets of a few nanometers [14,24,25].

(iv) In Eq. (23) we have supposed that the charge distribution in the double layer is not affected by the thermal gradient, i.e., we have neglected polarization effects; preliminary work [37] indicates that polarization corrections are of the order of λ/a and thus may safely be neglected for large particles.

B. Hydrodynamic boundary conditions

Comparison with the discussion of the charged double layer at the end of [31] reveals that Eq. (34) differs by a factor λ/a. This discrepancy arises from the boundary conditions for the velocity field at the solid-fluid interface. The present work is based on the no-slip boundary conditions (15), i.e., both tangential and normal components of the velocity are continuous, and in particular $\hat{v}_x(z=0)=0$ in Eq. (19). On the contrary, Ref. [31] uses perfect-slip conditions, corresponding to the reference value $\sigma_{xz}(0)=0$ of the surface stress,

$$\sigma_{xz}(z) = -\int_0^z dz' f_x, \tag{36}$$

instead of Eq. (18). Inserting the force field (12) one readily finds the stress on the fluid beyond the boundary layer, $\sigma_{xz}(\Lambda) = -(\sigma^2/4\varepsilon\lambda T)(1+\tau)\partial_x T$, which confirms Eq. (15) of [31]. The resulting expression for the Soret coefficient exceeds the present one by a factor a/λ. On the other hand, when evaluating the surface stress from Eq. (28) with the no-slip boundary velocity v_B, we find $\mathbf{n}\cdot\boldsymbol{\sigma}\cdot\mathbf{t} = -2\eta v_B/a$; inserting this in Eq. (6) of [31], one recovers the above results (32)–(34).

Thus the conditions of zero tangential velocity $[\hat{v}_x(0)=0]$ and zero shear stress $[\sigma_{xz}(0)=0]$ result in Soret coefficients that differ by a factor λ/a. This means that a much stronger Soret effect is expected for suspensions that satisfy slip boundary conditions, thus illustrating the importance of the properties of the particle-solvent interface. We note that the data on AOT-water-oil microemulsions, SDS micelles, and polystyrene nanoparticles [14,24,25] rather agree with the present result $S_T \propto a$ based on no-slip conditions, whereas those on micron-size polystyrene beads would match the law $S_T \propto a^2$ that follows from slip [20,21].

Available data suggest that significant slip may occur at hydrophobic interfaces [40], with slip lengths ranging from a few nanometers to a micron. Perfect slip as assumed in [31] occurs if the particle size is smaller than the slip length.

C. Previous theoretical work

Following Smoluchowski's argument for electrophoresis [38], Ruckenstein suggested a size-independent phoretic velocity u [22], implying a Soret coefficient $S_T \propto \lambda^2 a$, which was confirmed more recently by Refs. [26,27] and agrees with our Eq. (35). Regarding the prefactors, Refs. [22,27] discuss only the dominant behavior and do not account for the modified temperature gradient (13). Our result confirms that of Morozov [26] in the limit $\lambda \to 0$ and for weak coupling; we can make no statement concerning the negative Soret coefficient derived in [26] for strong charges.

More recent work took the thermal force as the gradient of the charging energy of the double layer [20,21,28–30]. This assumption results in dependencies of the Soret coefficient, $S_T \propto \lambda a^2$, that significantly differ from those given above. In order to point out the main differences, we rewrite Eq. (34) in terms of the charging energy $E_C = \frac{1}{2}Q\psi_0$; with the relation $\psi_0 = (Q/4\pi\varepsilon)(\lambda/a^2)$ one has

$$S_T = \frac{1}{T}\left(1 + \frac{\xi}{8}(1+\tau)\frac{\lambda}{a}\frac{Q\psi_0}{k_B T}\right). \tag{37}$$

Comparison with, e.g., Eq. (44) of [30] in the limit of thin boundary layers reveals that our expression is by a factor λ/a smaller than that obtained from the gradient of the charging energy.

The ratio ξ of thermal conductivities of solute and solvent is missing in most previous works. This factor ξ accounts for the local distortion of the temperature field $T(\mathbf{r})$; e.g., for example, if the particle is a good heat conductor, the temperature in its vicinity is almost constant, and its gradient is small. Depending on the thermal properties of solute and solvent, the factor ξ may considerably reduce the Soret effect [23]. Because of the high electronic heat conductivity, this effect has been discussed in particular for suspensions of metal particles [34].

Finally we note that the present approach differs from Derjaguin's model [39] which is based on enthalpy transport in a thermal gradient. This is most obvious when comparing the boundary velocity in Eq. (20) to the expression given in Chaps. 7 and 11 of [39] or in the review by Anderson [23].

D. Experiments

Available experimental findings [14,20,21,24,25] diverge with respect to the dependencies of the Soret coefficient on Debye length λ and particle size a. At present it is not clear whether the measured Soret effect varies linearly or with the square of the Debye length; see, e.g., the discussion in [14,30]. When comparing these measurements with the present or previous theoretical results, one should keep in mind that discrepancies could arise from the weak-charge assumption; it is by no means clear that the charged colloidal

systems discussed above satisfy the condition of weak coupling.

Regarding the dependence on the particle size a, very recent studies on AOT-water-oil microemulsions [24] and carboxyl functionalized polystyrene particles [25] show a linear dependence on the particle size, $S_T \propto a$, in the range of a few nanometers up to several tens of nm. Thus these experiments would agree with [22,27] and our Eq. (35) which is based on hydrodynamics with no-slip boundary conditions. On the other hand, a quadratic power law $S_T \propto a^2$ has been reported for polystyrene particles, where the radius ranges from $a=20$ nm to 1 micron, i.e., over almost two orders of magnitude [20,21]. Such a behavior has been obtained theoretically from the model based on the gradient of the charging energy [20,21,28–30], and from the boundary layer approach with perfect slip conditions [31].

ACKNOWLEDGMENTS

A.W. acknowledges stimulating and helpful discussions with R. Piazza, D. Braun, J. Dhont, and S. Wiegand.

[1] S. R. de Groot and P. Mazur, *Non-equilibrium Thermodynamics* (North-Holland, Amsterdam, 1962).
[2] J. C. Giddings, K. D. Caldwell, and M. N. Myers, Macromolecules **9**, 106 (1976); M. E. Schimpf and J. C. Giddings, *ibid.* **20**, 1561 (1987).
[3] M. Giglio and A. Vendramini, Phys. Rev. Lett. **38**, 26 (1977).
[4] *Thermal Nonequilibrium Phenomena in Fluid Mixtures*, edited by W. Köhler and S. Wiegand (Springer, Heidelberg, 2002).
[5] F. Zheng, Adv. Colloid Interface Sci. **77**, 255 (2002).
[6] A. Mohan and H. Brenner, Phys. Fluids **17**, 038107 (2005).
[7] D. R. Caldwell and S. A. Eide, Deep-Sea Res., Part A **28**, 1605 (1981); **32**, 965 (1985).
[8] L. L. Zheng, D. J. Larson, Jr., and H. Zhang, J. Cryst. Growth **191**, 243 (1998).
[9] K. J. Zhang, M. E. Briggs, R. W. Gammon, J. V. Sengers, and J. F. Douglas, J. Chem. Phys. **111**, 2270 (1999).
[10] J. Rauch and W. Köhler, Phys. Rev. Lett. **88**, 185901 (2002).
[11] J. Rauch and W. Köhler, Macromolecules **38**, 3571 (2005).
[12] S. Wiegand, J. Phys.: Condens. Matter **16**, R357 (2004).
[13] D. Braun and A. Libchaber, Phys. Rev. Lett. **89**, 188103 (2002); S. Duhr and D. Braun, *ibid.* **97**, 038103 (2006).
[14] R. Piazza and A. Guarino, Phys. Rev. Lett. **88**, 208302 (2002).
[15] S. Iacopini and R. Piazza, Europhys. Lett. **63**, 247 (2003).
[16] B.-J. de Gans, R. Kita, S. Wiegand, and J. Luettmer-Strathmann, Phys. Rev. Lett. **91**, 245501 (2003).
[17] R. Kita, S. Wiegand, and J. Luettmer-Strathmann, J. Chem. Phys. **121**, 3874 (2004).
[18] G. Demouchy, A. Mezulis, A. Bee, D. Talbot, J.-C. Bacri, and A. Bourdon, J. Phys. D **37**, 1417 (2004).
[19] S. Duhr and D. Braun, Appl. Phys. Lett. **86**, 131921 (2005).
[20] S. Duhr and D. Braun, Phys. Rev. Lett. **96**, 168301 (2006).
[21] S. Duhr and D. Braun, Proc. Natl. Acad. Sci. U.S.A. **103**, 19678 (2006).
[22] E. Ruckenstein, J. Colloid Interface Sci. **83**, 77 (1981).
[23] J. L. Anderson, Annu. Rev. Fluid Mech. **21**, 61 (1989).
[24] D. Vigolo, G. Brambilla, and R. Piazza, Phys. Rev. E **75**, 040401(R) (2007).
[25] S. A. Putnam, D. G. Cahill, and G. C. L. Wong, Langmuir **23**, 9221 (2007).
[26] K. I. Morozov, Zh. Eksp. Teor. Fiz. **115**, 1721 (1999); [JETP **88**, 944 (1999)].
[27] A. Parola and R. Piazza, Eur. Phys. J. E **15**, 255 (2004); J. Phys.: Condens. Matter **15**, S3639 (2005).
[28] E. Bringuier and A. Bourdon, Phys. Rev. E **67**, 011404 (2003).
[29] S. Fayolle, T. Bickel, S. Le Boiteux, and A. Würger, Phys. Rev. Lett. **95**, 208301 (2005).
[30] J. K. G. Dhont *et al.*, Langmuir **23**, 1674 (2007).
[31] A. Würger, Phys. Rev. Lett. **98**, 138301 (2007).
[32] J. A. Stratton, *Electromagnetic Theory* (McGraw-Hill, New York, 1941).
[33] L. D. Landau and E. M. Lifshitz, *Electrodynamics of Continuous Media* (Elsevier, Amsterdam, 1987).
[34] J. C. Giddings, P. M. Shinudu, and S. N. Semenov, J. Colloid Interface Sci. **176**, 454 (1995); P. M. Shiundu *et al.*, J. Chromatogr. **983**, 163 (2003).s
[35] L. D. Landau and E. M. Lifshitz, *Fluid Mechanics* (Elsevier, Amsterdam, 1987).
[36] L. Bocquet, E. Trizac, and M. Aubouy, J. Chem. Phys. **117**, 8138 (2002).
[37] J. K. G. Dhont and W. J. Briels (private communication).
[38] M. V. Smoluchowski, Z. Phys. Chem. **93**, 129 (1918).
[39] B. V. Derjaguin, N. V. Churaev, and V. M. Muller, *Surface Forces* (Plenum, New York, 1987).
[40] E. Lauga, M. P. Brenner, and H. A. Stone, in *Handbook of Experimental Fluid Dynamics*, edited by J. Foss *et al.* (Springer, New York, 2007)Chap. 19, pp. 1219–1240.